Data-driven Models for the Effects of Background Pressure on the Operation of Hall Thrusters

IEPC-2019-630

Presented at the 36th International Electric Propulsion Conference
University of Vienna, Austria
September 15–20, 2019

Matthew P. Byrne* and Benjamin A. Jorns†
University of Michigan, Ann Arbor, MI 48109

Data-driven models informed by a nested Markov chain Monte Carlo sampling approach are used to predict the thrust changes in an SPT-100 Hall effect thruster due to varying background pressure. The models are calibrated with parametric pressure data drawn from previous studies, and their results compared to previous thrust values. It is found that the data-driven phenomenological thrust model, while based only on predicted efficiencies, and not directly trained on thrust measurements, predicted thrust with better confidence than the empirical thrust model fit to the thrust changes alone. This is done to both improve the confidence in the model's predictions and to infuse some physics into an otherwise empirical process. The advantage of this data-driven probabilistic approach over traditional fitting stems from its ability to account for multiple sources of uncertainty, which typically limit the effectiveness of trend modeling. To validate the predictions of the model, the zero pressure thrust value is compared to experimental measurements of thrust on-orbit. The model predicts 79.1 mN ± 1.6 mN. The measured thrust of a similarly configured thruster on-orbit is 78.7 mN ± 1.3 mN. In addition to increased model fidelity, it is found that when measured total efficiency is compared to the total efficiency predicted by the model, that changes in divergence efficiency and voltage utilization efficiency account for the primary efficiency losses as backpressure is decreased. This result is discussed in the context of neutral ingestion and its impact on thruster efficiency.

*Ph.D Candidate, Department of Aerospace Engineering, mpbyrne@umich.edu
†Assistant Professor, Department of Aerospace Engineering

Nomenclature

HET	= Hall Effect Thruster
η_a	= Anode Efficiency
T	= Thrust
$\dot{m}$	= Mass Flow Rate
P_d	= Discharge Power
η_q	= Charge Utilization Efficiency
η_v	= Voltage Utilization Efficiency
η_d	= Divergence Efficiency
η_b	= Current Utilization Efficiency
η_m	= Mass Utilization Efficiency
V_{loss}	= Voltage Loss
V_d	= Discharge Voltage
δ	= Charge Weighted Divergence Angle
j	= Ion Current Density
θ	= Polar Angle
A_x, B_x, C_x	= Fitting Parameters
P	= Background Pressure

I. Introduction

Hall effect thrusters (HET) are becoming one of the most widely used electric propulsion technologies[1]. Yet, one of the major unanswered question about the operation of HETs is the validity of using ground measurements to predict the behavior of the thruster on-orbit. It is not yet possible to recreate true space conditions in the laboratory — at best base pressures six orders of magnitude higher than those in low-earth orbit can be achieved. This backpressure can have a significant effect on the operation of HETs, influencing key thruster properties such as thrust, plume divergence, cathode operation, and discharge current oscillations[2–18]. These effects are exacerbated for higher power thrusters which, due to their increased throughput, are subject to even higher pressures during testing. Given the trend in increasing HET power required to meet future mission needs, and in light the limitations of available pumping speed, there is a strong motivation to develop a method to map ground-based measurements to on-orbit behavior.

The standard method to address this problem is through parametric studies, systematically lowering the facility pressure to map the dependence of key thruster properties on backpressure[2–18]. Extrapolation then can be used to project measured trends to space-like pressures. While unambiguous in its implementation, there are a number of reservations with this method. For example, in order to perform an extrapolation, it is necessary to posit a functional dependence of the pressure (e.g., linear, exponential, quadratic, etc.). Absent a first-principles understanding of what drives facility effects, it is not clear what functional dependence of performance metrics, like thrust, is physically valid. Furthermore, even if there is a functional form that fits the measured data with high fidelity, it is not known if there is a valid way to extrapolate from the lowest pressure that can be achieved to flight-like conditions. Indeed, the only way to truly validate a functional form and its extrapolation is with in-space tests. These are prohibitively expensive. Faced with these limitations both in testing capability and knowledge of the physical processes, there is a pressing need to identify practical solutions that, at the minimum, allow us to rigorously quantify our confidence in the predictions of

an extrapolated model. It is important that we rigorously account for both measurement uncertainty (aleatory) and knowledge gaps in the physics (epistemic) so as to bound the predictions outside of the measurable pressure range.

Probabilistic studies are ideal methods for quantifying uncertainty, especially when tackling multi-dimensional problems with many possible sources of error. In these studies, model fitting parameters are treated as random variables which can vary according to a probability distribution function (PDF). These parameters are calibrated on experimental measurements and their PDFs are updated based on the new information. The goal of this study is to use this method to develop a data-driven model which can predict with uncertainty how the thrust of an SPT-100 Hall thruster will change under different backpressure conditions with a well defined confidence interval.

This paper is organized in the following way. In the first section we review the relevant facility effects and discuss the models and methods that we used to predict thruster operation at different background pressures. In the second section we present the calibrated fitting parameter PDFs generated by our probabilistic analyses. In the last section we discuss the predictions of our model and its relevance to future facility effect studies.

II. Theory and Approach

In this section we describe the methodologies used in predicting the performance changes in an SPT-100 Hall thruster as background pressure is decreased. We focus on predicting the changes in thrust based on changes in thruster efficiency.

A. Facility Effect Overview

There are major differences between the ground and flight environments experienced by HETs. These so-called facility effects have been shown to significantly alter the operation of HETs, and stem primarily from two unavoidable aspects of ground testing: the grounded chamber walls[17], and the finite background pressure. Of these, background pressure has been shown to have a substantial impact on thruster performance. The physical mechanisms behind how background neutrals alter thruster operation are convoluted at best, but there are four main effects which are active areas of research.

- **Neutral ingestion** The most direct way that the facility will impact thruster operation and thrust is through the direct ingestion of neutral gas from the environment. Neutrals can become entrained into the discharge channel, become ionized, and accelerate downstream. If left unaccounted for, these neutrals would cause a performance increase that would not be seen during flight. There are, however, a few studies[22,23] which show that this is likely a small contribution especially when compared to other facility effects. To mitigate this effect, most investigations operate thrusters at constant discharge power, reducing anode flow rate at higher background pressures to account for the additional discharge current generated by ingested background neutrals.
- **Stability** The effect of the facility of discharge current oscillations is both significant and poorly understood. Some studies have shown that oscillations increase with lowering background pressure[13], while others find that they decrease[2,3,5–8]. While understanding how thruster stability is altered by the background neutral density is critical to predicting how these devices will operated under different conditions, we confine this investigation to the more tractable averaged effects.
- **Cathode coupling** Cathode coupling has also been shown to be dependent on the background pressure of the chamber during thruster operation. While its effect on the discharge voltage is thought to be small, on the order of 1-2%[18], the cathode has been shown to play a role in

discharge oscillations changes[17] and the extent of the acceleration region[22,25,27]. In this report will will only account for its effect on voltage utilization.

- **Divergence angle** The final facility effect, and the primary subject of this study, is the trend of decreasing thrust with decreasing background pressure. This occurs even when the thruster is operated at constant power to control for neutral ingestion. This effect has obvious implications to the future development and use of these devices. If the thrust produced by a new thruster cannot be predicted accurately by ground testing, the increased risk may preclude their use on certain missions. The cause of this effect is thought to be changing acceleration region location which causes an increase in divergence at lower pressures. Supporting this theory are a number of studies documenting the movement of the acceleration region as a function of background pressure[7,24–26]. All of these experiments show that this effect is non-linear, they find small changes in thrust at higher pressures and large changes as the pressure drops below approx 20 $\mu Torr$.

B. Phenomenological Thrust Model

To predict how the thrust of a HET would change with different background pressures we used a phenomenological thrust model as described by Huang et al[5],

$$\eta_a = \frac{T^2}{2\dot{m}_a P_d} = \eta_q \eta_v \eta_d \eta_b \eta_m, \tag{1}$$

where η_a is the anode efficiency, T is the thrust, $\dot{m}_a$ is the anode mass flow rate, P_d is the discharge power, η_q is the charge utilization efficiency, η_v is the voltage utilization efficiency, η_d is the divergence efficiency, η_b is the current utilization efficiency, and η_m is the mass utilization efficiency.

This model was initially developed by Hofer[28] (from earlier work by Goebel and Katz[29]) to quantify the relative effects of different plasma properties. Using this model allows us to base our extrapolations on a firm physics foundation, even if we do not have a first-principles understanding for how each term is effected by background pressure. The mass utilization quantifies the amount of neutral mass flux that is converted to ion mass flux. The current utilization is determined by the amount of the discharge current that is made up of ion current. The voltage utilization efficiency details how much of the applied voltage goes into the acceleration potential. The charge utilization efficiency contains the losses due to multiply charged ions. Finally the divergence efficiency describes the thrust losses due to radial ion acceleration.

We focus our investigation on two of the efficiency terms, which we know will be affected by facility effects. Namely we look at the the voltage utilization efficiency (in which we assume that cathode coupling is the primary voltage loss mechanism[17,18]),

$$\eta_v = 1 - \frac{V_{cc}}{V_d}, \tag{2}$$

and the divergence efficiency,

$$\eta_d = < cos^2(\delta) >, \tag{3}$$

where V_{cc} is the cathode coupling voltage, V_d is the discharge voltage, and δ is the charge weighted divergence angle of the thruster plume. Divergence losses are, in a number of studies[2,4,5], pointed to as the dominant thrust loss mechanism for HET as background pressure is decreased. In this study we assume that all changes in efficiency are attributable to changes in these two terms holding all others constant.

C. Parametric Pressure Study

The data used to inform this study were taken from parametric pressure study performed by Diamant et.al.[2] on the SPT-100 thruster. The thruster used in this study was a flight model SPT-100 Hall thruster from the Fakel Experimental and Design Bureau. It was operated at 300 V and 1.35 kW in constant power mode. In this work, the effects of different background pressures on a SPT-100 performance and plasma properties were recorded at two different facilities. Of particular interest to this study are the calculations and measurements of thrust, efficiency, total mass flow rate, and ion flux sweeps. From this data Cusson et. al.[18] was able to extract values for cathode coupling voltage as it changed with respect to background pressure. We have plotted this data in Fig.1.

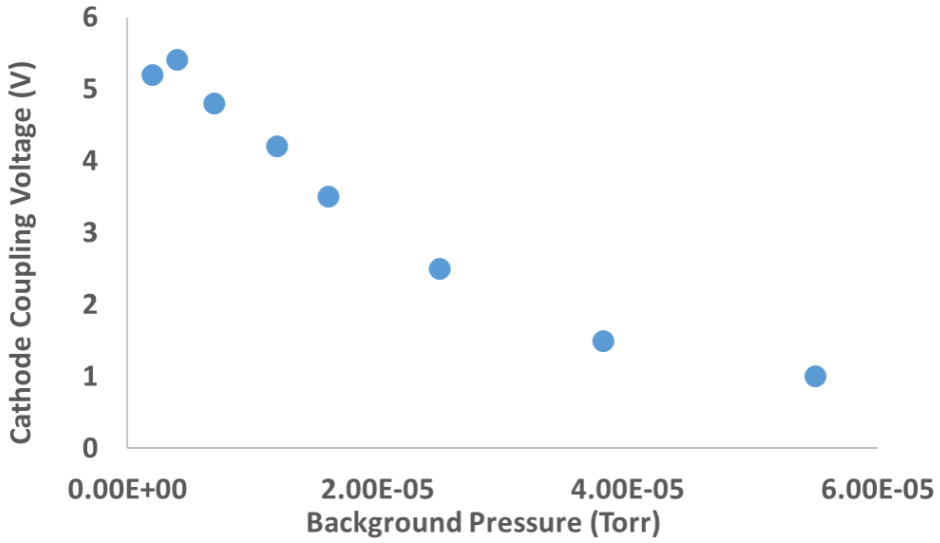

Fig. 1 Cathode coupling voltage as a function of background pressure extracted by Cusson et. al.[18] from Diamant et.at[2]

We extracted the divergence angle data from the ion flux sweeps performed by Diamant. We calculated the divergence angle based on the definition provided in Huang et. al.[4],

$$< cos\,(\delta) >= \frac{2\pi R_{FP}^2 \int_0^{\frac{\pi}{2}} j(\theta) cos(\theta) sin(\theta) d\theta}{2\pi R_{FP}^2 \int_0^{\frac{\pi}{2}} j(\theta) sin(\theta) d\theta}. \tag{4}$$

In this equation, δ is the charge weighted divergence angle, θ is the angle with respect to thruster centerline, and $j(\theta)$ is the ion current density as a function of angle from centerline. At the outer edges of the plume the the plasma properties of the beam are obscured by charge exchange ions which are not present during flight operation. These ions have different velocities than those originating from the beam. As a result, in order to calculate an accurate divergence angle it is necessary to remove the CEX wings[30]. This was done experimentally by Diamant by biasing the collection probe to exclude non-beam ions. We used the 100 V bias data to calculate divergence angle. The extracted data is plotted versus background pressure in Fig.2.

D. Bayesian Parameter Estimation Approach

Given the large amount of uncertainty in plume measurements, and the large number of relevant variables, a probabilistic Bayesian analysis is an ideal tool for finding the best fitting parameters while simultaneously quantifying the uncertainty. Bayesian Analysis is based on a theorem known as

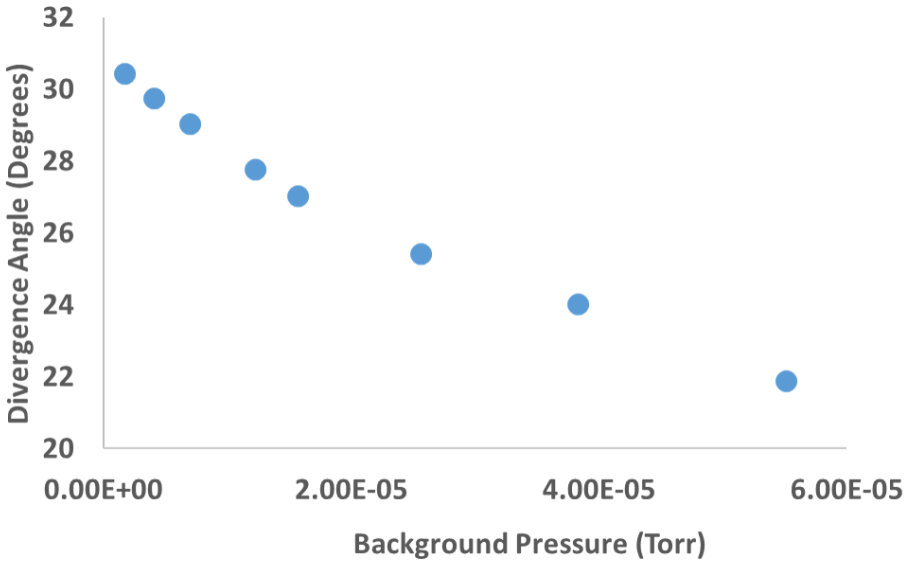

Fig. 2 Divergence angle as a function of background pressure, extracted from Diamant [2] RPA100 Ion Flux measurements at different background pressures

Bayes' rule,

$$P(\theta) = \frac{L(\theta) \cdot p(\theta)}{Z}, \tag{5}$$

where θ is a random variable, $p(\theta)$ is the prior probability distribution, $L(\theta)$ is the likelihood function, Z is the marginal likelihood or evidence, and $P(D)$ is the posterior probability distribution.

To apply this technique to our problem, first both of the efficiency terms noted above were assigned a fitting function which best describes its dependence on background pressure. Second each parameter in the fitting functions were assigned a pdf, known as a prior. Since we do not have any a priori information about the shape or range this distribution should have, we can represent our ignorance by selecting uniform distributions for each parameter. The third step is to choose a likelihood function. Most measured parameters naturally have a Gaussian distribution, and while it is true that some multiplicative processes are best described by more complicated likelihood choices[20,21], a Gaussian is the most straightforward choice for this study, given by,

$$L(\theta) = \frac{1}{2\pi\sigma} \cdot exp\left[-\frac{(\theta-\mu)^2}{2\sigma^2}\right], \tag{6}$$

where θ is a random variable, σ is the standard deviation of the distribution, and μ is the mean of the distribution. To put what these terms mean in the context of a measurement; μ would represent the true value of the quantity being measured (possibly given by a model), σ represents the chance that a different value is obtained when the quantity is measured, and θ is the value that you measured. The final step is to use the measured data and Bayes' Rule to perform a Bayesian update to redefine the ways each of the parameters are distributed. The resulting pdf is known as a posterior.

We generate the posteriors using a Nested Sampling Markov chain Monte Carlo (NSMCMC) approach. This process is described in detail by Sivia and Skilling[19], which we briefly review here. The algorithm begins by selecting a series of live points. Each live point is calculated by pulling a random sample of each fitting parameter prior. Each parameter set is then used to calculate a likelihood function. The lowest likelihood set is stored, and the parameters of that set are then re-assigned to a set with higher likelihood using an MCMC routine. This process is iterated approximately one

hundred thousand times (depending on how many live points are chosen) until the process converges on the set of parameters with the highest likelihood. Since we began with a uniform prior for each parameter, the corresponding posteriors are proportional to the calculated likelihood, from Bayes' Rule,

$$P(\theta) = \frac{L(\theta)}{Z} \propto L(\theta). \tag{7}$$

Since the value of each parameter now has an associated pdf based on the underlying data and its uncertainty, we can "propagate" that uncertainty through the calculations and ultimately to our predictions. For each fitting function we can then Monte Carlo sample each parameter to find the complete range of values that fitting function can take. Confidence intervals can then be drawn to provide an uncertainty envelope.

III. Results and Analysis

In this section we will display the results of our parameter estimation study. First, we will describe the models we chose and the reasons behind their selection. Second, we will examine the results of our Bayesian parameter estimation technique. Finally we will use those results to make thrust predictions for on-orbit pressures. We will also compare our thrust predictions and Diamant's to experimental measurements of thrust from the Russian express missions[31].

A. Model Selection

- **Cathode Coupling Model**
  To model the cathode coupling voltage as a function of background pressure, we chose an exponential of the form,

$$V_{cc}(P) = A_{V_{cc}} \cdot exp\left(B_{V_{cc}} \cdot P\right), \tag{8}$$

  where $A_{V_{cc}}$ and $B_{V_{cc}}$ are fitting parameters. We chose this form based on the work done by Cusson[18]. In this paper they propose a first principles model for the change in cathode coupling as a function of neutral density. While their model fits the data very well, it is very complicated. Therefore, for this study we used a simpler equation of the same form with two fit parameters.
- **Divergence Angle Model**
  Unlike the cathode coupling model, when fitting the divergence angle data we did not use a physics-based model, as no such model exists. Instead we used a polynomial model. We selected a quadratic model given by

$$\delta(P) = A_\delta P^2 \cdot B_\delta P \cdot C_\delta, \tag{9}$$

  where A_δ, B_δ, and C_δ are fitting parameters. We chose quadratic because it was the lowest possible order polynomial that still qualitatively matched the data. While this assumption allows us to proceed with the probabilistic analysis, it restricts the applicability of the results to the SPT-100 only, since other thrusters may have different functional forms.
- **Phenomenological Thrust Model**
  Based on the assumptions we introduced above, we can rewrite the phenomenological thrust model(equation 1) in terms of its backpressure dependence,

$$T(P) = \sqrt{\dot{m}_a \cdot C \cdot \left(1 - \frac{V_{cc}(P)}{V_d}\right) \cdot cos^2\left(\delta(P)\right)}, \tag{10}$$

  where

$$C = P_d \cdot \eta_q \cdot \eta_b \cdot \eta_m. \tag{11}$$

We calculate C based on the Diamant's[2] average reported values for total efficiency, thrust, and mass flow rate at $5 \cdot 10^{-5}$ Torr.

- **Diamant's Thrust Model**
  Diamant has an empirical model which was fit to experimental thrust measurements, shown in Fig.3 with the parameter values chosen by Diamant. To have a point of comparison for our phenomenological model predictions, we also applied the parameter estimation technique to Diamant's model given by,

$$T_{Diam}(P) = A_T - B_T \cdot exp\left(-C_T \cdot P\right), \tag{12}$$

where A_T, B_T, and C_T are fitting parameters.

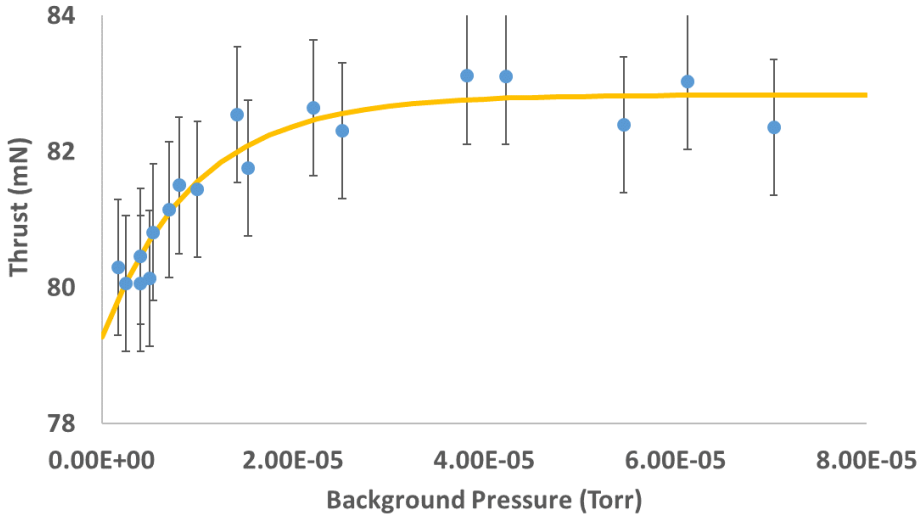

Fig. 3 Thrust measurements as a function background pressure extracted from Diamant[2] (Blue), and Diamant's fit (Yellow)

B. Bayesian Parameter Estimation Results

The results of the parameter estimation study are displayed in this section. In Figs. 4, 5, and 6 we show the posterior distributions for each fitting parameter of the models we selected in the previous section. The plots on the left side of each figure are the individual posterior distributions for each fitting parameter. The heat plots on right side of the figures are the joint probability distributions between the two of the fitting parameters in each model.

Beginning with the results for the cathode coupling model (Equation 8), shown in Fig.4, we can see that both fitting parameters are very well defined. Each parameter has standard deviations one order of magnitude lower than their mean. This is not surprising considering that we chose this model based on a first-principles model for the cathode coupling. The last feature of note is the clear covariance in the parameters, indicated by the slope in the joint distribution function. This suggests that the values of $A_{V_{cc}}$ and $B_{V_{cc}}$ are correlated. This will lead to less model uncertainty in regions where the model is not supported by experimental data.

In Fig.5, we see the parameter estimation results for the divergence angle model (Equation 9) . Similar to the cathode coupling fits we have well defined posteriors for each fit parameter. But unlike

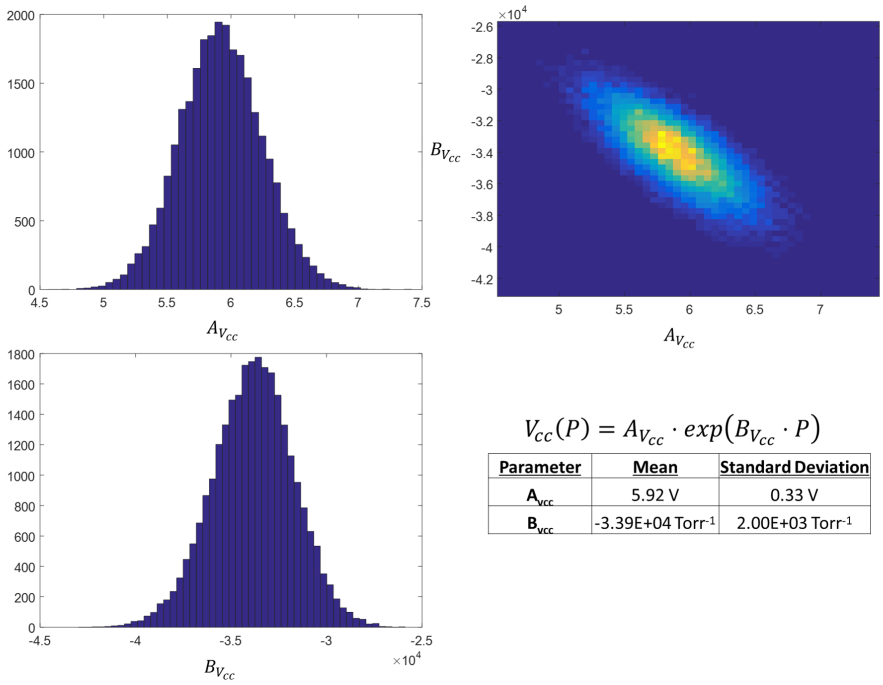

Parameter	Mean	Standard Deviation
A_{vcc}	5.92 V	0.33 V
B_{vcc}	-3.39E+04 Torr^{-1}	2.00E+03 Torr^{-1}

Fig. 4 Posterior probability distributions for the cathode coupling fitting parameters.

for the cathode coupling values, these values have very large standard deviation (on the same order as the mean). This relative increase in the standard deviation is expected in higher dimensional models, as the extra degrees of freedom allow the number if likely values to increase. Despite this, we can see from the joint probability distributions that all of the parameters are correlated to each other.

We also calibrated Diamant's empirical thrust model (Equation 12) on the thrust data published by Diamant[2]. The resulting posteriors are displayed in Fig.6. We find that only the A_T posterior is well defined. The B_T posterior, while it seems to be well peaked, has a large standard deviation. The last parameter, C_T, has a very broad posterior. This indicates that it is an unstable parameter, that when it is not informed by data, will blow up. Furthermore, when both it and B_T were allowed to vary together, the parameter estimation could not converge on any values for either parameter. This can be seen in the joint probability distribution for B_T and C_T. At low values of B_T and C_T the probability is high, but if either is increased the other becomes nearly uniform.

C. Probabilistic Predictions

We can use the posterior distributions fitting parameters to make predictions with uncertainty. This can be done by calculating fits using all the possible combinations of fit parameters. Since the posterior distributions are essentially sets of the most probable values that each fitting parameter can take, we need only sample values from these distributions to approximate all of the probable fit functions. The uncertainty of the posteriors (which was initially based on the uncertainty of the data) can be propagated through this calculation as fits using unlikely parameters will themselves be unlikely. It is also in this way that we can assess the uncertainty of regions where we have no experimental data. The set of all possible fitting functions is restricted by the data we do have, allowing us to then restrict what values possible new data points are likely to take.

As an example we can apply this method using the posteriors calculated to for Diamant's empirical thrust model. We begin by randomly sampling a value from each of the posteriors shown in Fig. 6.

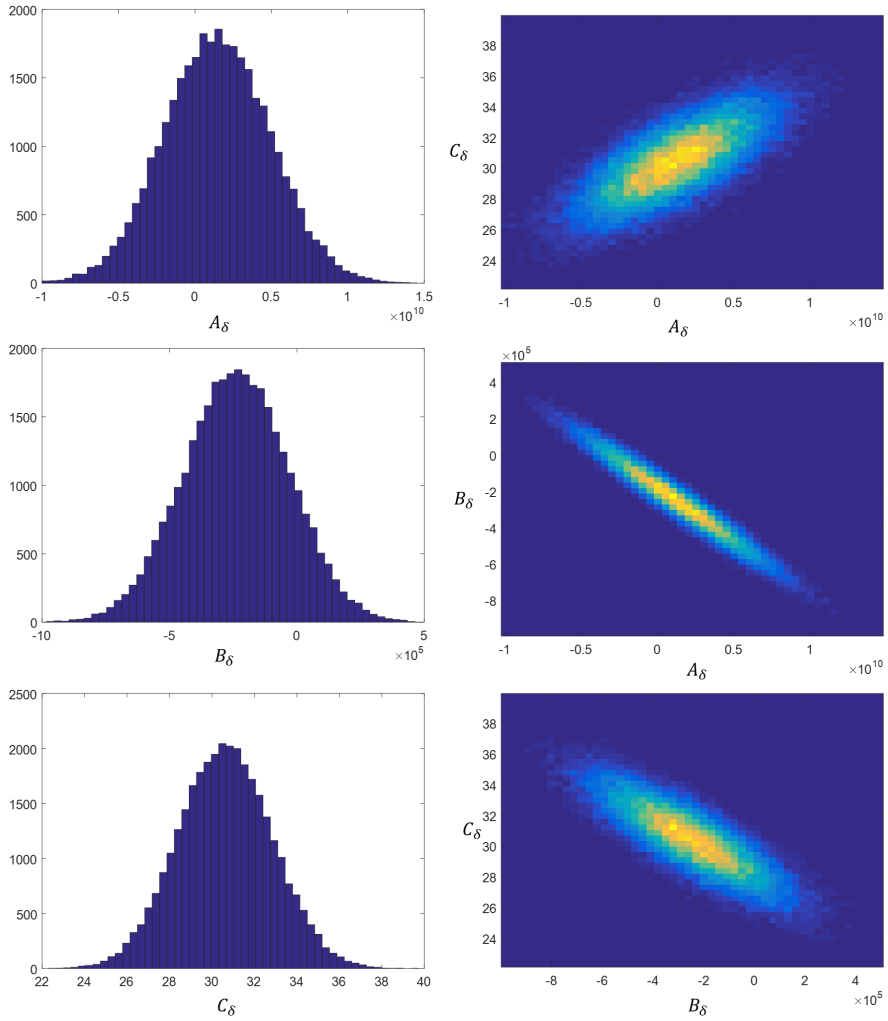

$$\delta(P) = A_\delta \cdot P^2 + B_\delta \cdot P + C_\delta$$

Parameter	Mean	Standard Deviation
$\mathbf{A_\delta}$	1.49E+09 Deg/Torr^2	3.47E+09 Deg/Torr^2
$\mathbf{B_\delta}$	-2.37E+05 Deg/Torr	2.07E+05 Deg/Torr
$\mathbf{C_\delta}$	30.63 Deg	2.11 Deg

Fig. 5 Posterior probability distributions for the divergence angle fitting parameters.

These values are then input into equation 12 and used to calculate a fit function. The outputs of the fit function are then stored. This process is repeated ten thousand times. At each pressure value, each of the ten thousand models is compiled to create a PDF of thrust values at that point. This is done at all pressure points and used to calculate the mean and confidence intervals plotted in Fig.7.

In this plot we can see that the mean fits the available data well. Furthermore, where there is data the the confidence intervals are close to the mean, indicating low uncertainty. Conversely, where there is no data support, the confidence intervals immediately diverge from the mean. This is a consequence of the high uncertainty and low correlation between the models fit parameters.

We apply the same algorithm to the divergence and cathode coupling data. We propagate the uncertainty from the posteriors through each model, but this time we take the additional step of propagating each models results through our phenomenological thrust model. This outcome of this can be seen in Fig.8. For this plot the mass flow rate values are chosen based on Diamant's mass flow

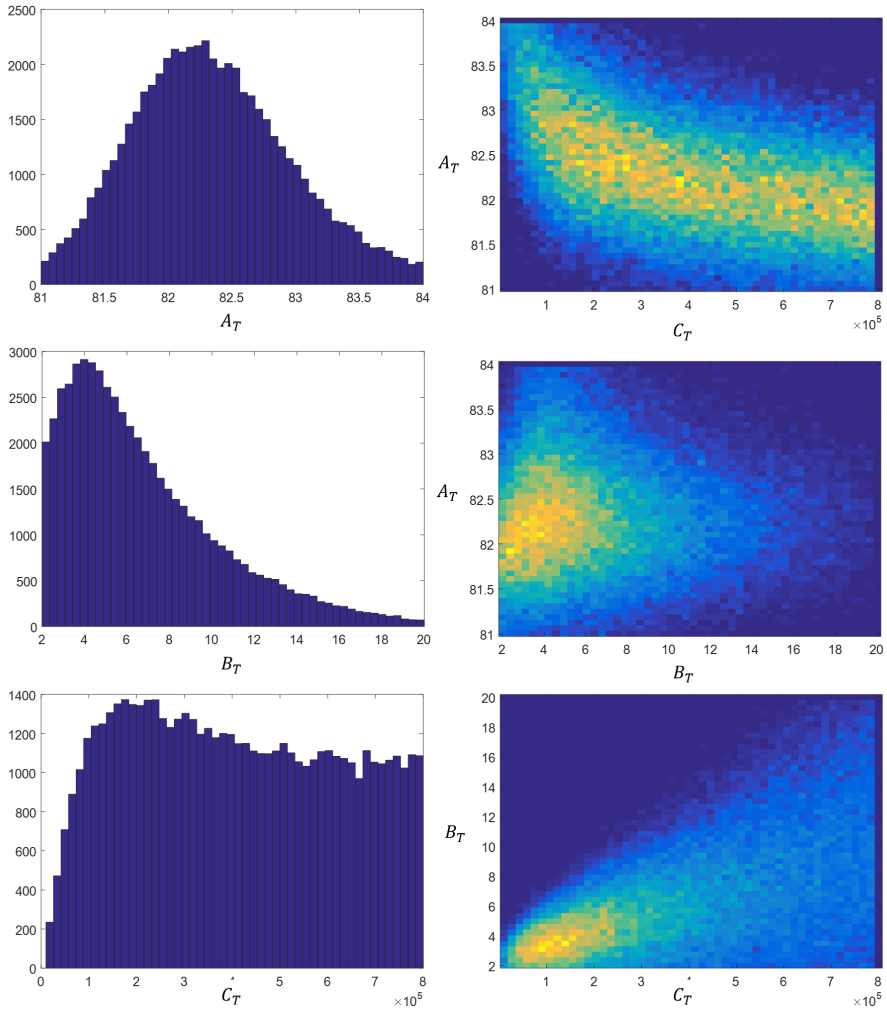

$$T_{Diam}(P) = A_T - B_T \cdot exp(-C_T \cdot P)$$

Parameter	Mean	Standard Deviation
A_T	82.34 mN	0.61 mN
B_T	6.81 mN	3.67 mN
C_T	4.06E+05 Torr^{-1}	2.17E+05 Torr^{-1}

Fig. 6 Posterior probability distributions for the divergence angle fitting parameters.

rate fit,

$$\dot{m} = 5.68 - 7728 \cdot P. \tag{13}$$

When we explore the fitting results we see immediately that the mean matches the experimentally measured thrust values very well. Additionally all of the data points fall within the confidence intervals. However, unlike the Diamant's model, this model was not trained on the thrust data itself. To see why the fit matched the data so well we examine how the predicted total efficiency changes with respect to background pressure, and how it compares to the measured total efficiency. We calculate total efficiency through the equation,

$$\eta_a = \eta_q \eta_v \eta_d \eta_b \eta_m = \eta_{constant} \cdot \left(1 - \frac{V_{cc}(P)}{V_d}\right) \cdot cos^2\left(\delta(P)\right), \tag{14}$$

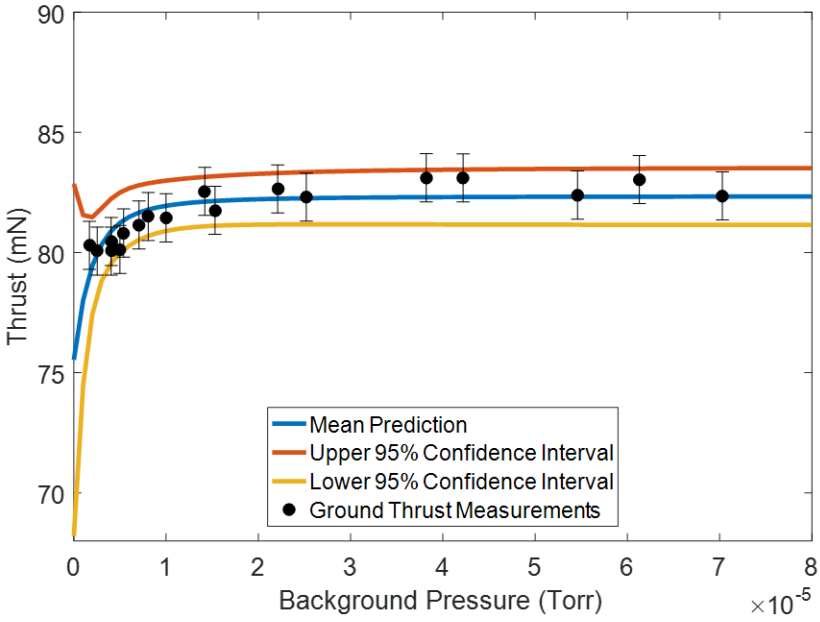

Fig. 7 Diamant's Thrust Predictions with 95% confidence intervals. Plotted with experimental thrust data for context

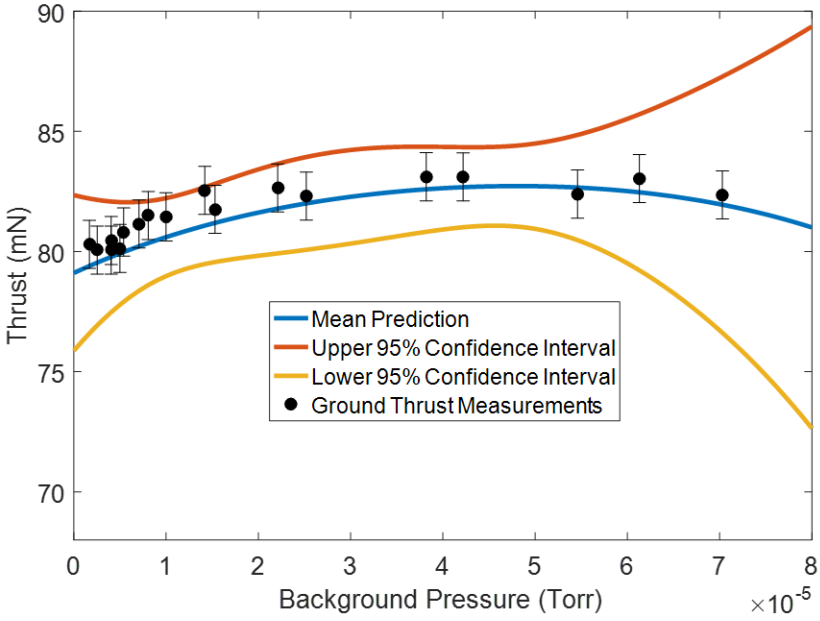

Fig. 8 Phenomenological Thrust Predictions with 95% confidence intervals. Plotted with experimental thrust data for context.

where $\eta_{constant} = 0.5644$ and was calculated for a particular value of η_a at $5 \cdot 10^{-5}$ Torr and held constant for all pressures. The results are plotted in Fig.9, we can see that even only letting divergence and voltage utilization efficiencies vary, the predictions match very well with experimental measurements.

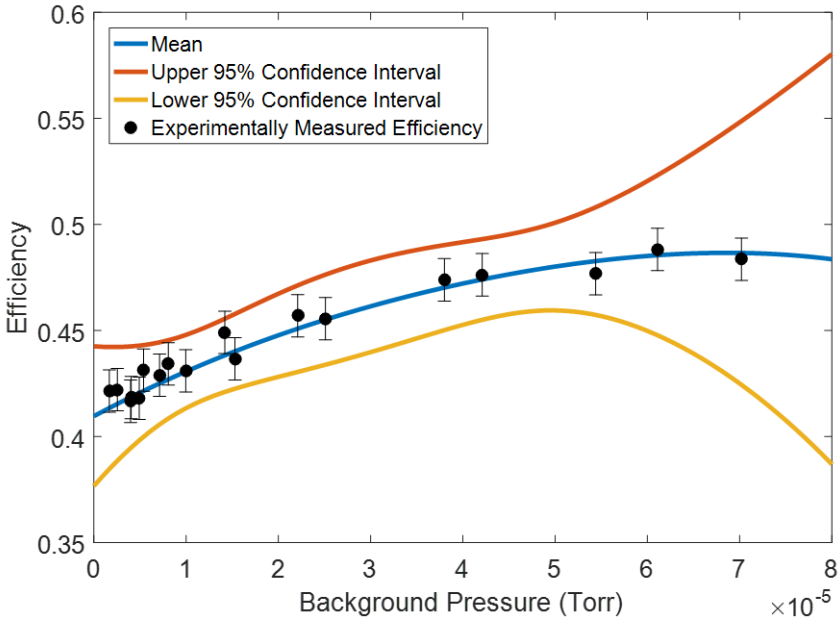

Fig. 9 Predicted and measured total efficiency as a function of changing background pressure.

D. Comparison to Orbital Measurements

Thrust measurements of an SPT-100 have been performed on-orbit.[31] In the year 2000, two Russian geosynchronous communication satellites were launched into orbit. Each satellite was equipped with eight Fakel Enterprises SPT-100 Hall thrusters, as well as a number of plasma diagnostic systems. The thrust of some of the devices was able to be calculated during the final orbital corrections of the spacecraft, as well as during station keeping burns. From this data set, we selected thrust measurements from thrusters which had fired for at least 1.5 times the manufacturer suggested burn-in time of 20 hours[31](Express-A#2: RT2 and Express-A#3: RT1,T4, and RT4) to ensure a better comparison to the well-worn thruster analyzed by Diamant[2]. We then corrected for the higher voltage and current measured on orbit and averaged the thrust from all four thrusters to give some indication of the reliability of this number. The average measured thrust was found to be 78.7 mN $\pm$ 1.3 mN.

We can compare this number to what is predicted by our two models. Figure 10 shows how this orbital value compares to the predictions of the phenomenological model. We can see that the mean predicted value agrees with the measured orbital thrust number to withing the variance if the data. If we calculate the mean and standard deviation of the model predictions at zero pressure, we find that the model predicts 79.1 mN $\pm$ 1.6 mN.

For context on the importance of this result we can look at how the predictions of Diamant's model compare to the orbital data. Figure 11 shows this comparison. We observe that while the model's confidence bounds encompass the data point, the mean predictions do not seem to match. At zero pressure the mean and standard deviation of the predictions is 75.5 mN $\pm$ 3.74 mN.

IV. Discussion

In this section we discuss the results generated by our parameter estimation technique, and its benefits over traditional fitting techniques. The most obvious difference between the two methods can be seen by comparing Figs. 3 and 7. Whereas the traditional fitting method captures the same

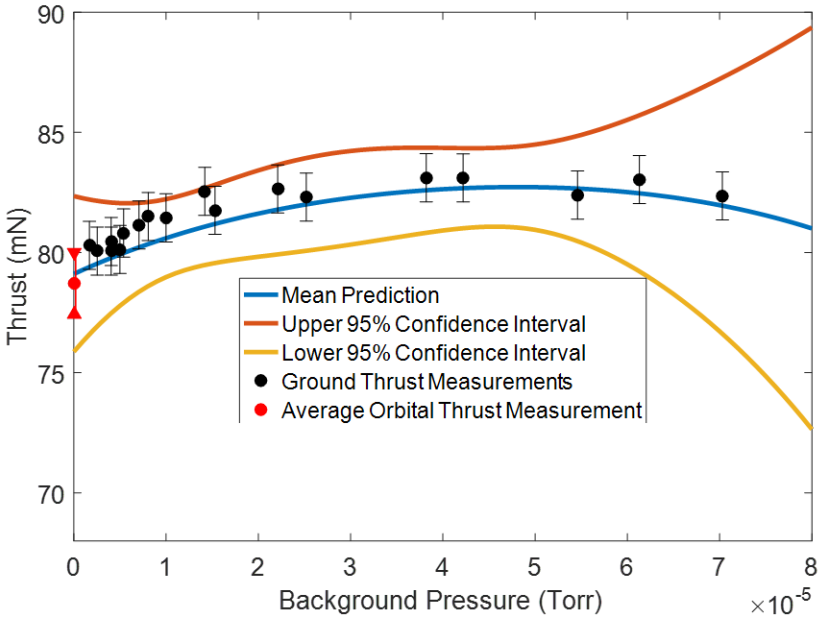

Fig. 10 Phenomenological Thrust Predictions with 95% confidence intervals. Plotted with orbital thrust data from Russian Express Missions[31]

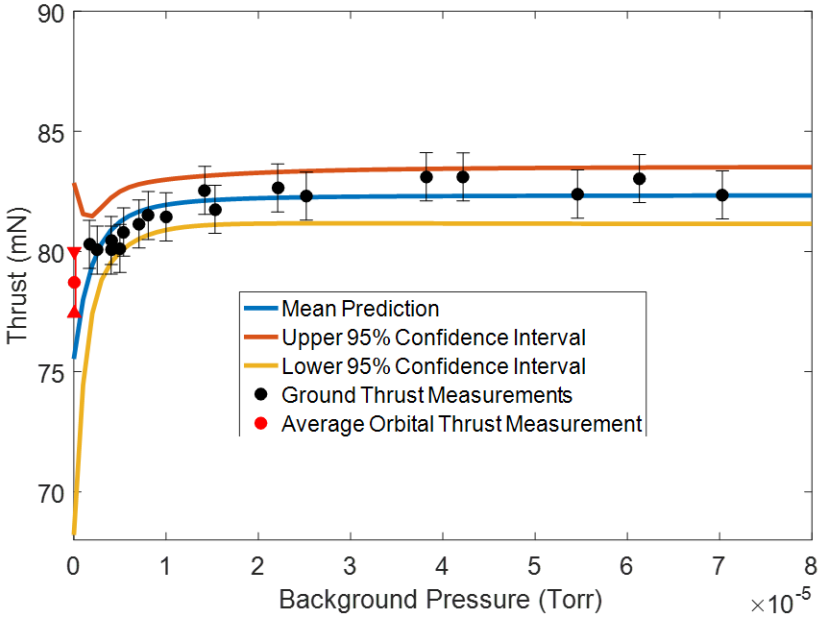

Fig. 11 Diamant's Thrust Predictions with 95% confidence intervals. Plotted with orbital thrust data from Russian Express Missions[31]

trend in the data, it gives no indication for how certain that fit is. While it is possible to measure how good a fit is with non-Bayesian methods, like root mean square estimation, in most cases all of the data points are given equal weight. In the Bayesian case, parameters are treated as random variables which can vary. As a result, it can more easily deal with data outliers since confidence intervals are

based on the resulting posterior PDFs.

There was another interesting development of this study. When we look at how total efficiency changes with background pressure we find that, accounting for only changes in divergence angle and voltage utilization, that we match the experimentally measured values. This is a surprising result considering that we are not taking into account neutral ingestion. Diamant ran the thruster in constant power mode and was forced to increase the anode flow rate to maintain constant power as the backpressure was reduced. If we assume that neutral ingestion is making up for the difference in mass flow by holding $\dot{m}$ constant at the predicted zero pressure value, we see that the predicted thrust matches at low pressure but is much greater at higher pressures. This is shown in Fig.12.

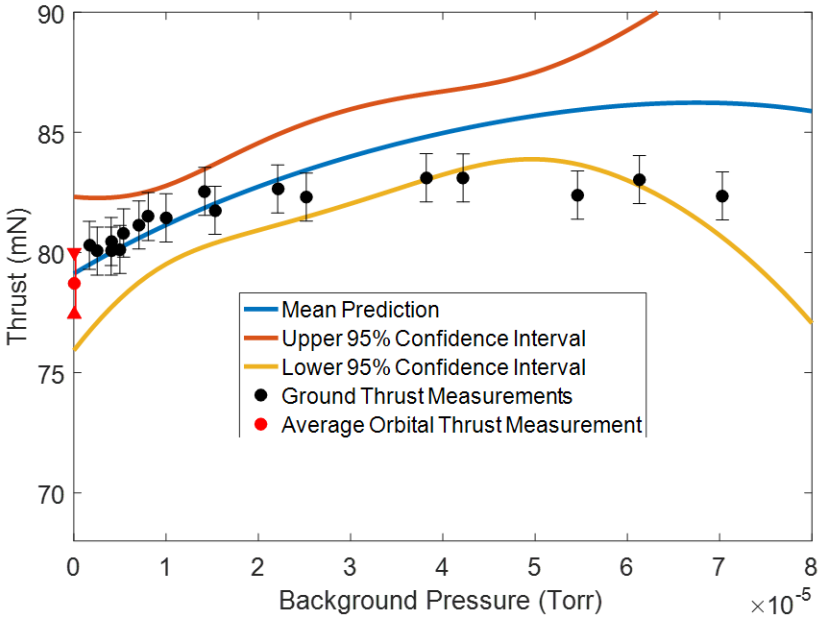

Fig. 12 Phenomenological Thrust Predictions with 95% confidence intervals. $\dot{m} = 5.68$ **mg/s**

Since do to neutral ingestion we must lower anode flow rate to maintain constant power, it may indicate that at higher pressures the mass utilization efficiency increases since current will be generated by background neutrals not considered in the measured mass flow rate. However, since the trend in total efficiency appeared to be completely explained by the change in divergence efficiency, one (or more) of the others we held constant must be dropping to compensate. We surmise that the voltage utilization efficiency is dropping due to a new (unaccounted for) loss term. If it is indeed due to neutral ingestion as we suspect, the likely effect is that these neutrals are not being ionized at the same potential as anode-supplied neutrals. This leads to the same measured current and power, but less thrust. This observation does not change the result of our modeling, since background neutrals will likely play a minor role at orbital pressures.

The final accomplishment of this paper is the ability of the phenomenological model to predict the thrust produced at orbital pressures within the variance of the on-orbit measurements. The most probable value predicted by the model was 79.1 mN, which is less than 1 mN for the avereage measured value of 78.7 mN. Additionally, the inclusion of a physical basis reduced the width of the confidence intervals when compared to the empirical model suggested by Diamant[2]. In the future we can further improve the confidence of our predictions by including both more efficiency terms, such as mass utilization, and more physics-based functional forms for how the terms should vary with

background pressure.

In addition to thrust, studies like this could easily be expanded to predict the changes of any plume parameter with respect varying background pressure. One hope is that they can be used to bound predictions of plasma plume properties near spacecraft surfaces on orbit.. This could have interesting implications for spacecraft integration. If the plume can be well predicted in-space, the effect of ion sputtering on spacecraft materials on orbit could be more rigorously calculated.

V. Conclusions

We used a data-driven Bayesian parameter estimation technique on a phenomenological thrust model to predict changes in thrust as a function of background pressure with a well-defined uncertainty envelope. Further, we found that the dominant effects driving thruster efficiency loss as background pressure decreased, are reduced divergence and voltage utilization efficiencies. Additionally, we found that while neutral ingestion does not play a role at lower pressures, there is a possibility that it can lead to decreased thrust at higher pressures when thrusters are run in constant power mode. Finally, we found that our most probable prediction of thrust at orbital pressures matched the thrust of an SPT-100 Hall thruster measured on-orbit to within 1 mN.

References

[1] Hart, W. , Lev, D., Myers, R., Kolbeck, J., Keidar, M., Gonzalez, J., Choe, W., Koizumi, H., Albertoni, R., Gabriel, S., and Funaki, I. "The Technological and Commercial Expansion of Electric Propulsion in the Past 24 Years." presented at the 35th International Electric Propulsion Conference, Georgia Institute of Technology, USA, 2017, vol. IEPC-2017-242

[2] Diamant K. D., Liang R., and Corey R. L. "The E□ect of Background Pressure on SPT-100 Hall Thruster Performance", 50th AIAA/ASME/SAE/ASEE Joint Propulsion Conference, AIAA Propulsion and Energy Forum, (AIAA 2014-3710)

[3] Diamant, K. D., Spektor, R., Beiting, E. J., Young, J. A., and Curtiss, T. J., "The E□ects of Background Pressure on Hall Thruster Operation," in 48th AIAA/ASME/SAE/ASEE Joint Propulsion Conference and Exhibit, Atlanta, Georgia, USA, AIAA-3735-2012.

[4] Huang, W., Kamhawi, H., and Haag, T., "E□ect of Background Pressure on the Performance and Plume of the HiVHAc Hall Thruster," Presented at the 33rd International Electric Propulsion Conference, IEPC Paper 2013-058, Washington, DC, Oct 6-10, 2013.

[5] Huang, W. , Kamhawi, H., and Haag, T. "Facility E□ect Characterization Test of NASA's HERMeS Hall Thruster", 52nd AIAA/SAE/ASEE Joint Propulsion Conference, AIAA Propulsion and Energy Forum, (AIAA 2016-4828)

[6] Byers, D. and Dankanich, J. W., "A Review of Facility E□ects on Hall E□ect Thrusters," Presented at the 31st International Electric Propulsion Conference, IEPC Paper 2009-076, Ann Arbor, MI, Sept. 20-24, 2009.

[7] MacDonald-Tenenbaum, N., Pratt, Q., Nakles, M., Pilgram, N., Holmes, M., and Hargus Jr, W., "Background Pressure E□ects on Ion Velocity Distributions in an SPT-100 Hall Thruster," Journal of Propulsion and Power, Vol. 35, No. 2, 2019, pp. 403–412.

[8] Nakles, M., and Hargus, W "Background Pressure E□ects on Ion Velocity Distribution Within a Medium-Power Hall Thruster," JOURNAL OF PROPULSION AND POWER Vol. 27, No. 4, July–August 2011

[9] M. L. R. Walker, "E□ects of facility backpressure on the performance and plume of a Hall thruster," Ph.D. thesis (United States Air Force, 2005).

[10] Brown, D.L. and Gallimore, A.D., "Evaluation of facility e□ects on ion migration in a Hall thruster plume." Journal of Propulsion and Power 27, no. 3 (2011): 573-585.

[11] R. Spektor, W. G. Tighe, H. Stoltz, K. R. C. Beckwith, “Facility E□ects on Hall Thruster Performance Through Cathode Coupling,” Presented at Joint Conference of 30th International Symposium on Space Technology and Science, 34th International Electric Propulsion Conference and 6th Nano-satellite Symposium, Hyogo-Kobe, Japan, July 4–10, 2015, IEPC-2015-309/ISTS-2015-b-309

[12] Randolph, T., Kim, V., Kaufman, H., Kozubsky, K., Zhurin, V.V. and Day, M., "Facility e□ects on stationary plasma thruster testing." in Proceedings of the 23rd International Electric Propulsion Conference (1993), pp. 1993–1093.

[13] Snyder, J.S., Lenguito, G., Frieman, J.D., Haag, T.W. and Mackey, J.A., “The E□ects of Background Pressure on SPT-140 Thruster Performance at Multiple Power Levels,” 53rd AIAA/ASME/SAE/ASEE Joint Propulsion Conference, July 9-11, 2018, Cincinnati, OH

[14] Kamhawi, H., Huang, W., Haag, T. and Spektor, R., “Investigation of the E□ects of Facility Background Pressure on the Performance and Voltage-Current Characteristics of the High Voltage Hall Accelerator,” in Proceedings of the 50th AIAA/ASME/SAE/ASEE Joint Propulsion Conference (2014), p. 3707

[15] Hofer, R.R., Peterson, P.Y. and Gallimore, A.D., “Characterizing Vacuum Facility Backpressure E□ects on the Performance of a Hall Thruster,” in Proceedings of the 27th International Electric Propulsion Conference, IEPC-01-045, Pasadena, CA (2001).

[16] Manzella, D. , Jankovsky, R., Elliott, F. , Mikellides, I., Jongeward, G., and Allen, D., “Hall Thruster Plume Measurements On-Board the Russian Express Satellites,” presented at the 27th International Electric Propulsion Conference, Pasadena, California, 2001.

[17] Frieman, J.D., Walker, J.A., Walker, M.L., Khayms, V. and King, D.Q., "Electrical facility e□ects on Hall thruster cathode coupling: performance and plume properties." Journal of Propulsion and Power 32, no. 1 (2015): 251-264.

[18] Cusson, S. E., Jorns, B., and Gallimore, A., "Simple Model for Cathode Coupling Voltage Versus Background Pressure in a Hall Thruster," 53rd AIAA/SAE/ASEE Joint Propulsion Conference, 10-12 July 2017, Atlanta, GA, AIAA 2017-4889

[19] Sivia, D. S., and Skilling, J., Data Analysis: A Bayesian Tutorial, 2nd edition, Oxford University Press, 2006

[20] Yim, J., “A survey of xenon ion sputter yield data and fits relevant to electric propulsion spacecraft integration,” presented at the 35th International Electric Propulsion Conference, Georgia Institute of Technology, USA, 2017, vol. IEPC-2017-060.

[21] Limpert, E., Stahel, W.A. and Abbt, M.,Limpert, Eckhard, Werner A. Stahel, and Markus Abbt. "Log-normal distributions across the sciences: keys and clues: on the charms of statistics, and how mechanical models resembling gambling machines o□er a link to a handy way to characterize log-normal distributions, which can provide deeper insight into variability and probability—normal or log-normal: that is the question." BioScience 51, no. 5 (2001): 341-352.

[22] Cusson, S. E., Georgin, M. P., Dragnea, H. C., Dale, E. T., Dhaliwal, V., Boyd, I. D., and Gallimore, A. D., “On channel interactions in nested Hall thrusters,” Journal of Applied Physics 123:13

[23] Frieman, J. D., Liu, T. M., and Walker, M. L. R., “Background Flow Model of Hall Thruster Neutral Ingestion,”. JOURNAL OF PROPULSION AND POWER. Vol. 33, No. 5, September–October 2017

[24] Cusson, S. E., Dale, E. T., Jorns, B. A., and Gallimore, A. D., “Impact of Cathode Flow Fraction on the Location of the Acceleration Region,” SPC-18-402

[25] Cusson, S.E., Byrne, M., Jorns, B., and Gallimore, A. "Investigation into the Use of Cathode Flow Fraction to Mitigate Pressure-Related Facility E□ects on a Magnetically Shielded Hall Thruster," AIAA Propulsion and Energy 2019 Forum, Indianapolis, IN, AIAA-2019-4077, August 19-22, 2019

[26] Cusson, S. E., Dale, E. T., Jorns, B. A., and Gallimore, A. D., “Acceleration Region Dynamics in a Magnetically Shielded Hall Thruster,” Phys. Plasmas 26, 023506 (2019);

[27] Georgin, M. P., Dahliwal, V., and Gallimore, A. D., “Investigation of Channel Interactions in a Nested Hall Thruster Part I: Acceleration Region Velocimetry,” 52nd AIAA/SAE/ASEE Joint Propulsion Conference. July 25-27, 2016, Salt Lake City, UT

[28] Hofer, R. R,"Development and Characterization of High-E□ciency, High-Specific Impulse Xenon Hall Thrusters," University of Michigan, Ph.D. Dissertation, 2004

[29] Goebel, D. M., and Katz, I. Fundamentals of electric propulsion: ion and Hall thrusters. Vol. 1. John Wiley and Sons, 2008.

[30] Huang, W., Shastry, R., Herman, D. A., Soulas, G. C., and Kamhawi, H., "Ion Current Density Study of the NASA-300M and NASA-457Mv2 Hall Thrusters", 48th AIAA/ASME/SAE/ASEE Joint Propulsion Conference and Exhibit, AIAA-2012-3870, Atlanta, GA, 29 Jul.- 1 Aug., 2012.

[31] Manzella, D. H., Jankovsky, R., Elliott, F., Mikellides, I., Jongeward, G., and Alien, D., "Hall Thruster Plume Measurements On-Board the Russian Express Satellites," IEPC Paper 2001-044, October 2001.